Self-similar singularity formation in 2D inextensible string

James Cross
Stony Brook University
Stony Brook, New York
james.cross@stonybrook.edu

August 19, 2025

Abstract

The dynamics of a thin, periodic segment of string constrained to a plane are captured by a closed plane curve in its arc length parametrization with a 'no-stretch' constraint and an equation of motion derived from a variational principle. By the method of Lagrange multipliers, the constraint is enforced by the variable tension throughout the string. Numerics show finite-time blow up through a self-similar mechanism. We reproduce and add to the existing body of numerical work by approximating the string with a discrete chain and simulating dynamics with an explicit Euler method. Additionally, basic properties of the tension, curvature, and vorticity of the string are proven with techniques learned in a first semester undergraduate analysis course and were found consistent with the simulation.

Contents

1 Introduction

The initial value-boundary value problem of a thin inextensible string constrained to a plane has been studied before for its similarities to the Euler equations governing incompressible fluids in work done by Thess et al. [7]. As stated there, both systems have a constraint enforcing a constant measure, are derived from a variational principle, and are governed by non-linear partial differential equations. Such similarities lead even to definitions of 'vorticity' on a string and comparisons of the finite-time curvature blow up to vortex stretching in fluids by Thess et al. In the same spirit, we define 'enstrophy' on the string as well.

This write-up studies the case for periodic boundary conditions. The case of one free end and one fixed end corresponding to a whip have been studied extensively before by Preston in a series of papers [4, 5, 1]. Therewithin, Preston proved that the motion of the chain approximates the motion of the whip (Section 7.1) and the existence and uniqueness of solutions for times $[0, t)$ (Theorem 7.5) in [4]. While we do not show these here directly, we rely on the result to draw conclusions about the string from the chain simulation. We find basic analytical results for the tension, curvature, and vorticity, which were found to be consistent with the simulation despite it being an explicit first order method.

Section 1.1 introduces the basic equations and quantities of the system. Section 1.2, specifically, defines curvature and vorticity for the string and discusses some results about them with tension. Section 2 reviews the apparent self-similar behavior driving the blow up seen in the numerics here and Thess et al. [7]. Section 3 discusses possible post-blow up evolution and the results of running the chain simulation past the blow up time. Section A is the appendix containing the longer derivations, the details of the numerical scheme using Preston's chain approximation [4], and energy conservation.

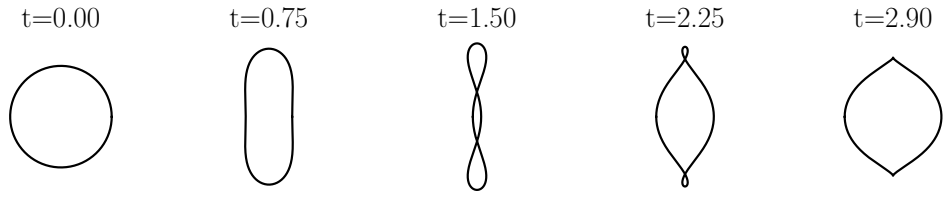

Figure 1: To-scale evolution of unit length periodic chain at times $t = 0$, 0.75, 1.5, 2.25, and 2.9 with initial position $x(s, 0) = \cos(s)e_x + \sin(s)e_y$ and initial velocity $\partial_t x(s, 0) = -2/30 \cos^3(s)e_x + 2/30 \sin^3(s)e_y$ by a numerical simulation.

1.1 The system

The inextensible periodic string is described by the following system of equations.

Fix a time $T > 0$. Consider a map $x : [0,1) \times [0,T) \to \mathbb{R}^2$, whose image is periodic $x(s,t) = x(s+1,t)$ of length 1 with variable tension $\sigma : [0,1) \times [0,T) \to \mathbb{R}$, $\sigma(s,t) = \sigma(s+1,t)$. The string is inextensible

$$\|\partial_s x(s,t)\|^2 = 1, \tag{1}$$

and evolves according to its equation of motion

$$\partial_{tt} x(s,t) = \partial_s \left(\sigma(s,t)\partial_s x(s,t)\right). \tag{2}$$

$\|\cdot\|$ denotes the standard norm on $\mathbb{R}^2$, and s is an arc length parametrization of the curve. A derivation of (2) with the Lagrangian formalism of classical mechanics is provided in the appendix A.

Expanding the equation of motion expresses the force in an orthogonal basis where forces along the length of the string $\partial_s x$ correspond to nonuniformity of the tension and forces perpendicular to the string $\partial_{ss} x$ correspond to the size of the tension and curvature as later defined.

$$\partial_{tt} x(s,t) = \partial_s \sigma(s,t)\partial_s x(s,t) + \sigma(s,t)\partial_{ss} x(s,t) \tag{3}$$

Using the constraint (1) and the equation of motion (2), one can show that the tension σ solves a linear ordinary differential equation.

$$-\partial_{ss}\sigma(s,t) + \|\partial_{ss} x(s,t)\|^2 \sigma(s,t) = \|\partial_{st} x\|^2 \tag{4}$$

In the following section, we rewrite this equation with vorticity and curvature to obtain results about the tension.

1.2 Tension, curvature, and vorticity

Given that the string is arc length parametrized $x(s,t)$, it is reasonable to define curvature $k : [0,1) \times [0,T) \to \mathbb{R}^2$ as

$$k(s,t) \coloneqq \partial_s x^{\perp}(s,t) \cdot \partial_{ss} x(s,t), \tag{5}$$

since $\partial_s x \cdot \partial_{ss} x = 0$.

To study the evolution of the tangent vector $\partial_s x$, we can define vorticity $\omega : [0,1) \times [0,T) \to \mathbb{R}^2$ as

$$\omega(s,t) \coloneqq \partial_s x^{\perp}(s,t) \cdot \partial_{st} x(s,t). \tag{6}$$

like in Thess et al. [7], since $\partial_s x \cdot \partial_{st} x = 0$, similar to curvature.

Curvature and vorticity are also equivalently thought of as how much the angle ϕ of the tangent vector $\partial_s x = (\cos(\phi), \sin(\phi))$ changes in s and t, respectively.

$$k = \partial_s \phi \qquad \omega = \partial_t \phi \tag{7}$$

It then follows that $\partial_t k = \partial_s \omega$ and that the total curvature in a C^2 string is constant, $\partial_t \int_0^1 k ds = 0$.

For the initial position of a closed regular curve the total curvature is a constant $2\pi n$ where n is the rotation index defined by equation (31), since the continuous tangent vector must start and end the string with the same angle modulo 2π. In particular for a circle, the total curvature is 2π.

These geometric quantities determine the dynamics through the tension σ. We see in Proposition 1 that σ solves an ordinary differential equation governed by ω and k.

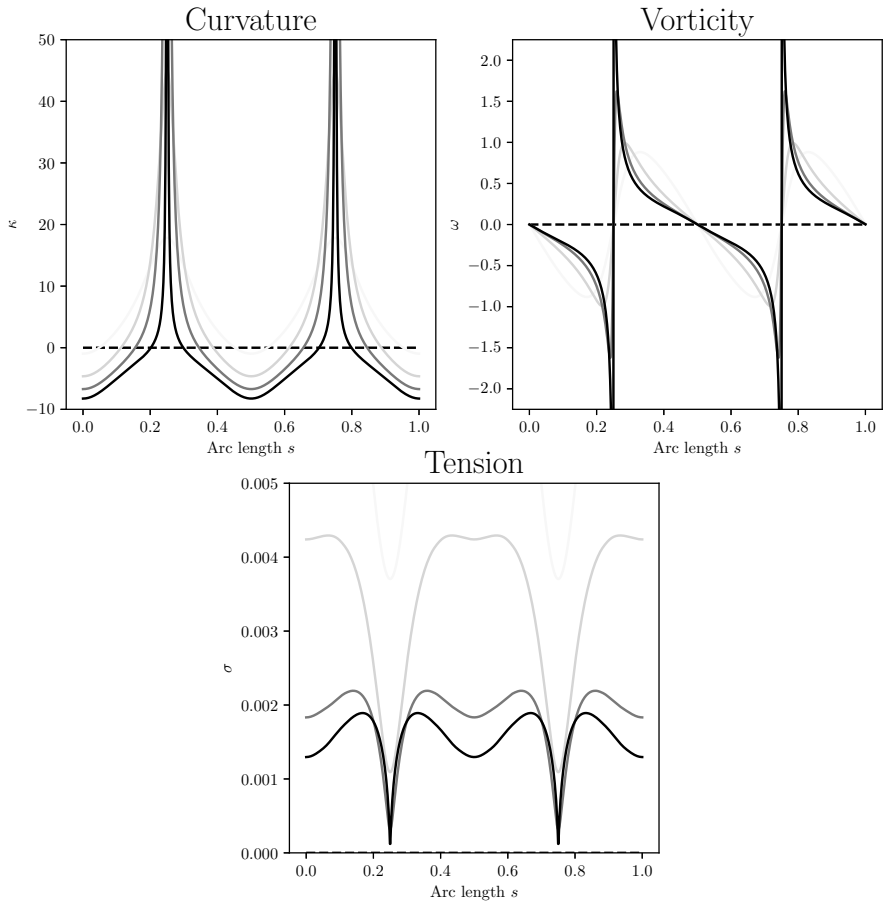

Figure 2: Curvature k, vorticity ω, and tension σ throughout a unit length chain at $t = 0.0$, 0.75, 1.50, 2.25, and 2.90 in light-to-dark order from the chain simulation (M=1000 links). Curvature and vorticity plots are cut off to show the detail at times farther from the blow up time. $s = 0.25$ and $s = 0.75$ correspond to the top and bottom tips of the string in the simulation respectively.

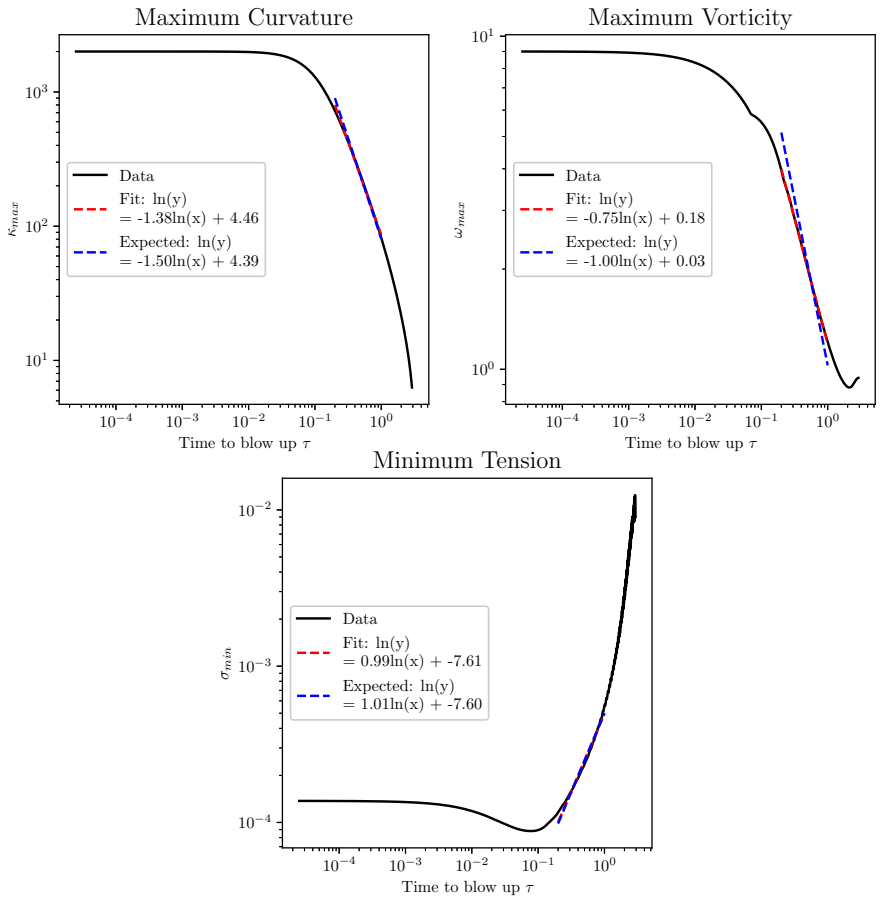

Figure 3: Maximum curvature $|k|_{\max}$, maximum vorticity $\omega_{\max}$, and minimum tension $\sigma_{\min}$ throughout a unit length chain plotted against remaining time to blow up τ fitted after the appearance of self-similarity and before loss of resolution (M=1000 links). Based on self-similar formulas for curvature (22), vorticity (23), and tension (24) at $\beta = 3/2$, the fitted slopes deviate from their expected values by curvature 7.7%, vorticity -12.9%, and tension -1%.

1.2.1 Tension equation

Proposition 1. *For any point $s \in [0,1)$ and time $t \in [0,T)$ on the string,*

$$(-\partial_{ss} + [k(s,t)]^2)\sigma(s,t) = [\omega(s,t)]^2 . \tag{8}$$

Proof. Start with the equation of motion (2), and expand it.

$$\begin{aligned} \partial_{tt}x &= \partial_s(\sigma\partial_s x) \\ &= \partial_s\sigma\partial_s x + \sigma\partial_{ss}x \end{aligned}$$

Take ∂_s and then the dot product with $\partial_s x$.

$$\begin{aligned} \partial_{stt}x &= \partial_{ss}\sigma\partial_s x + 2\partial_s\sigma\partial_{ss}x + \sigma\partial_{sss}x \\ \partial_s x \cdot \partial_{stt}x &= \partial_s x \cdot (\partial_{ss}\sigma\partial_s x + 2\partial_s\sigma\partial_{ss}x + \sigma\partial_{sss}x) \end{aligned}$$

Using the constraint (1), one can simplify the dot products

$$\begin{aligned} \|\partial_s x\|^2 = 1 \overset{\partial_s}{\Longrightarrow} \partial_s x \cdot \partial_{ss}x = 0 \overset{\partial_s}{\Longrightarrow} \partial_s x \cdot \partial_{sss}x = -\|\partial_{ss}x\|^2 \\ \|\partial_s x\|^2 = 1 \overset{\partial_{tt}}{\Longrightarrow} \partial_s x \cdot \partial_{stt}x = -\|\partial_{st}x\|^2 \end{aligned}$$

Substituting in these relations recovers the tension equation

$$\begin{aligned} -\|\partial_{st}x\|^2 &= \partial_{ss}\sigma - \|\partial_{ss}x\|^2\sigma \\ -\partial_{ss}\sigma + \|\partial_{ss}x\|^2\sigma &= \|\partial_{st}x\|^2 \end{aligned}$$

By definition of curvature and vorticity as, we restate the equation

$$(-\partial_{ss} + k^2)\sigma = \omega^2$$

and complete the derivation. □

This equation and the following already known fact are vital for proving the following results of this section.

1.2.2 Positivity of tension

Theorem 1. *Fix a time $t \in [0,T)$. If $x(\cdot,t) : [0,1) \to \mathbb{R}^2$ and $\sigma(\cdot,t) : [0,1) \to \mathbb{R}$ are continuous and $\exists s \in [0,1),\ k(s,t) \neq 0$, then $\forall s \in [0,1)$*

$$\sigma(s,t) > 0. \tag{9}$$

Proof. Here we show $\sigma(s,t) \geq 0$. Let $t \in \mathbb{R}$ be fixed. By the extreme value theorem,

$$\exists s' \in [0,1) \text{ s.t. } \sigma(s',t) = \min_{s\in[0,1)} [\sigma(s,t)].$$

Now, the second derivative at s' must be non-negative $\partial_{ss}\sigma(s',t) \geq 0$ because $\sigma(s',t)$ is a minimum. It follows from (8) at s' that

$$\begin{aligned} & -\partial_{ss}\sigma(s',t) + k(s',t)^2\sigma(s',t) = \omega(s',t)^2 \\ \Rightarrow \quad & -\partial_{ss}\sigma(s',t) + k(s',t)^2\sigma(s',t) \geq 0 && (10) \\ \Rightarrow \quad & 0 \leq \partial_{ss}\sigma(s',t) \leq k(s',t)^2\sigma(s',t) && (11) \end{aligned}$$

Therefore, $\sigma(s',t)$ is non-negative. By the minimality of $\sigma(s',t)$, $\sigma(s,t)$ is also non-negative. Therefore, $\forall t \in [0,T)$ if $\sigma(s,t)$ is continuous in s on $[0,1)$, then $\sigma(s,t)$ is non-negative $\forall s \in [0,1)$.

See Proposition A.2 in [5] for a proof of the existence of the Green's function $G : [0,1) \times [0,1) \times [0,T) \to \mathbb{R}$ that solves

$$\begin{aligned} & -\partial_{ss}G(s,s',t) + k(s,t)^2 G(s,s') = \delta(s-s') \\ & G(0,s',t) = G(1,s',t), \qquad \partial_s G(0,s',t) = \partial_s G(1,s',t). \end{aligned}$$

By construction, it follows that

$$\sigma(s,t) = \int_0^1 G(s,s',t)\omega(s,t)^2 ds'.$$

Proposition A.3 then gives a positive lower bound on it if the curvature is not identically 0, from which $\sigma(s) > 0$ immediately follows. □

In [6] and [4] respectively, Shnirelman and Preston credit Victor Yudovich for showing but not publishing early results, such as this one on the positivity of tension.

1.2.3 Convexity and concavity of tension

Proposition 2. *Fix $t \in [0,T)$ and $s \in [0,1)$. If $\omega(s,t) = 0$, then $\partial_{ss}\sigma(s,t) \geq 0$. If $k(s,t) = 0$, then $\partial_{ss}\sigma(s,t) \leq 0$. Restated, the tension is convex at vorticity zeros and concave at curvature zeros.*

Proof. Recall the tension equation (8), and let $t_0 \in [0,T), s_0 \in [0,1]$ such that $\omega(s_0,t_0) = 0$.

$$-\partial_{ss}\sigma(s_0,t_0) + k(s_0,t_0)^2\sigma(s_0,t_0) = \omega(s_0,t_0)^2 = 0$$

By the non-negativity of the tension in result 1,

$$\partial_{ss}\sigma(s_0,t_0) = k(s_0,t_0)^2\sigma(s_0,t_0) \geq 0 \tag{12}$$

Therefore, σ is convex in s around s_0 when $\omega(s_0,t_0) = 0$.

Let $t_1 \in [0,T)$ and $s_1 \in [0,1)$ such that $k(s_1,t_1) = 0$.

$$-\partial_{ss}\sigma(s_1,t_1) + k(s_1,t_1)^2\sigma(s_1,t_1) = \omega(s_1,t_1)^2 \tag{13}$$

$$\partial_{ss}\sigma(s_1,t_1) = -\omega(s_1,t_1)^2 \leq 0 \tag{14}$$

Therefore, σ is concave in s around s_1 when $k(s_1,t_1) = 0$. □

From this, we can say that vorticity zeros $\omega = 0$ correspond to convex regions of the tension σ, and inflection points $k = |k| = \|\partial_{ss}x\| = 0$ in the string correspond to concave regions of the tension σ.

We can also integrate in s between points $a, b \in [0,1)$ where $\partial_s\sigma(b,t) - \partial_s\sigma(a,t) = 0$ for some fixed $t > 0$.

1.2.4 Enstrophy

Let $\mathcal{E}([a,b],t) \coloneqq \int_a^b |\omega(s,t)|^2\, ds$ be called the enstrophy in $[a,b] \subset S^1$ at time $t > 0$.

Proposition 3. *Fix $t \in [0,T)$. $\mathcal{E}([0,1),t) = \int_0^1 k(s,t)^2\sigma(s,t)ds$.*

Proof. The proof follows immediately from the fundamental theorem of calculus and periodicity of the tension and its first derivative $\partial_s\sigma$.

$$\int_0^1 -\partial_{ss}\sigma(s,t) + k(s,t)^2\sigma(s,t)ds = \int_0^1 \omega(s,t)^2 ds \tag{15}$$

$$\Rightarrow \mathcal{E}([0,1),t) = \int_0^1 k(s,t)^2\sigma(s,t)ds \tag{16}$$

□

The enstrophy can thus be interpreted as the weighted L^2-norm of the curvature by the tension since the tension is positive by Proposition 1.

Proposition 4. *Fix $t \in [0,T)$. If $a, b \in S^1$ are locations of tension extrema $\partial_s\sigma(a) = \partial_s\sigma(b) = 0$, then $\mathcal{E}([a,b],t) = \int_a^b k(s,t)^2\sigma(s,t)ds$.*

Proof. The proof follows from the fundamental theorem of calculus. □

1.3 Inflection points

The classification of the singularity comes down to it being either a corner or a cusp. The distinction comes down to if the tangent vectors approaching the point from either side are merely discontinuous or entirely antiparallel of each other.

One way for a corner to form is by two inflection points approaching each other in the limit with discontinuous tangent vectors. If a pair of inflection points s_-, s_+ where $\partial_s k(s_-,t) < 0 < \partial_s k(s_-,t)$ meet in the limit, they can do so either 'peacefully' like when a bend in a curve is pulled out or collide 'violently' like when a knot is cinched tightly. While more complex behaviors may be possible, these two simple cases can be illustrative.

We can describe the motion of the inflection points s_+ and s_- using the implicit function theorem [3].

Proposition 5. *Suppose $x \in C^3$, and $(s_0,t_0) \in [0,1) \times [0,T)$ such that $k(s_0,t_0) = 0,\ \partial_s k(s_0,t_0) \neq 0$. Then $\exists I \subset [0,T)$ open, $t_0 \in I$, $\exists S_0 : I \to [0,1),\ S_0 \in C^1$ such that $S_0(t_0) = s_0$ and $\forall t \in I$*

$$k(S_0(t),t) = 0,\ \partial_s k(S_0(t),t) \neq 0. \tag{17}$$

Furthermore,

$$\frac{d}{dt}S_0(t) = -\frac{\partial_t k(S_0(t),t)}{\partial_s k(S_0(t),t)}\ . \tag{18}$$

Proof. Recall that curvature is given by the map $k : [0,1)\times[0,T) \to \mathbb{R}, (s,t) \mapsto \partial_s x^\perp(s,t) \cdot \partial_{ss}x(s,t)$. By hypothesis $x \in C^3$, and this implies that $k \in C^1$. The given point (s_0,t_0) meets the criteria for the implicit function theorem

$$k(s_0,t_0) = 0,\ \partial_s k(s_0,t_0) \neq 0. \tag{19}$$

This gives us the first part of the proposition that parametrizes a given inflection point. The second part of the proposition follows from theorem 9.1 in [3]. □

These observations are all geometric. The question remains if the dynamics, the behavior of σ and the equation of motion (2), yield such a case where k grows between the inflection points.

In the numerics that follow, we see that such a case may be possible when the string passes through itself to create self-intersecting loops.

2 Self-similarity

In Figure 4 from the simulation, a loop structure forms in the string after self-intersection and appears to shrink uniformly in the plane up to some critical time. In Thess et al., this self-similar behavior was described, and we reproduce it between Sections 2.1 and 2.2. Furthermore, we propose a certain profile for the self-similar loop and analyze the profile in Section 2.3.

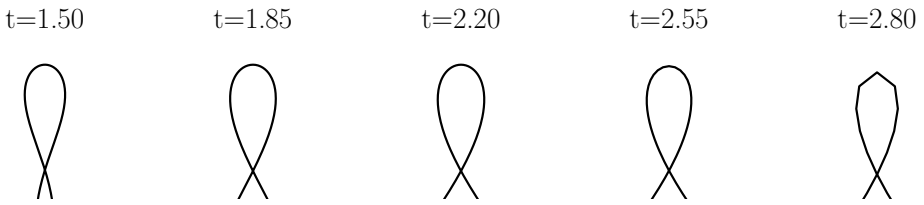

Figure 4: Rescaled view of the evolution of the loop between the blow up point and the self-intersection point. Each successive image is scaled down from the last until the resolution becomes coarse just before the blow up.

In Thess et al., the self-similar function is the angle of the tangent vector, ϕ.

Let $T > 0$ be the blow up time, $\tau = T - t$ the time until blow up, and $\partial_s x(s,t) = \cos(\phi(s,t))e_x + \sin(\phi(s,t))e_y$ the tangent vector. For all s, t, this tangent vector obeys the no stretch constraint (1).

$$\phi(s,t) = \tau^\alpha f\left(\frac{s}{\tau^\beta}\right) \tag{20}$$

$$\sigma(s,t) = \tau^\gamma g\left(\frac{s}{\tau^\beta}\right) \tag{21}$$

Thess et al. showed that by applying equations (2) and (8), one finds that $\alpha = 0$ and $\gamma = 2\beta - 2$ in order for the evolution to be self-similar.

Recall that by definition, vorticity and curvature are $\omega = \partial_t \phi$ and $k = \partial_s \phi$. From this, one should expect to find the following self-similar functions of $\xi = s\tau^{-\beta}$ around the eventual singular point $s = 0$ by compensating with some power of τ:

$$\tau^\beta k(s,t) = f'(\xi) \tag{22}$$

$$\tau\omega(s,t) = \beta\xi f'(\xi) \tag{23}$$

$$\tau^{2-2\beta}\sigma(s,t) = g(\xi) \tag{24}$$

2.1 Numerics

Thess et al. uses a numerical shooting method to show β can be near $3/2$. This justifies scanning around $\beta = 3/2$ to calculate the compensated quantities from equations (23), (22), and (24). We found that $\beta = 1.581$ optimized vorticity and $\beta = 1.529$ optimized tension for orthogonal distance to their fit lines. No $\beta \in [1, 2]$ optimized curvature. However, this is entirely unproblematic because the range of residuals between different β's is very small, only 0.0064. See the Figure 6 in Section 2.2 for more details about the optimized β's. The plots for $\beta = 1.500$ are pictured below.

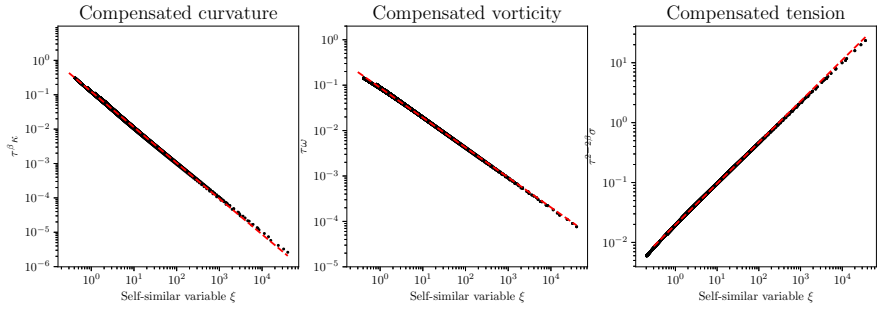

Figure 5: Log-log plots of compensated curvature $\tau^\beta k$ (left), compensated vorticity $\tau\omega$ (middle), and compensated tension $\tau^{2-2\beta}\sigma$ (right) against the self-similar variable $\xi = s\tau^{-\beta}$, where $\beta = 3/2$, from the numerical simulation. The data shown is only for five links left and right of the blow up link ($M = 1000$ links) for times $t = 2.89$ up until the blow up time $T = 2.90815$. The fitted red, dashed lines have slopes of -1.038 ± 0.015 (curvature), -0.659 ± 0.009 (vorticity), and 0.688 ± 0.009 (tension) on the fitted region.

The fact that the quantities came out as lines when plotted against $|\xi|$ on the loglog plot supports the idea that the compensated versions of curvature, vorticity, and tension are self-similar quantities for a particular regime of ξ. Additionally, the slopes of the lines of best fit suggest their scaling to leading order up to multiplication by a constant.

2.2 Optimizing β

When justifying the estimate of β, we made several plots of the quantities on the region of $3 \cdot 10^{-1} \leq \xi \leq 4 \cdot 10^4$ where they appeared self-similar and measured the orthogonal distance of each point from the fit line. To get the 'normalized residual,' we then divided by the number of points in the region in order for this measure to not depend on the number of points in the region.

This worked for vorticity and tension where there are clear minima in the region, but curvature had no such obvious minimum.

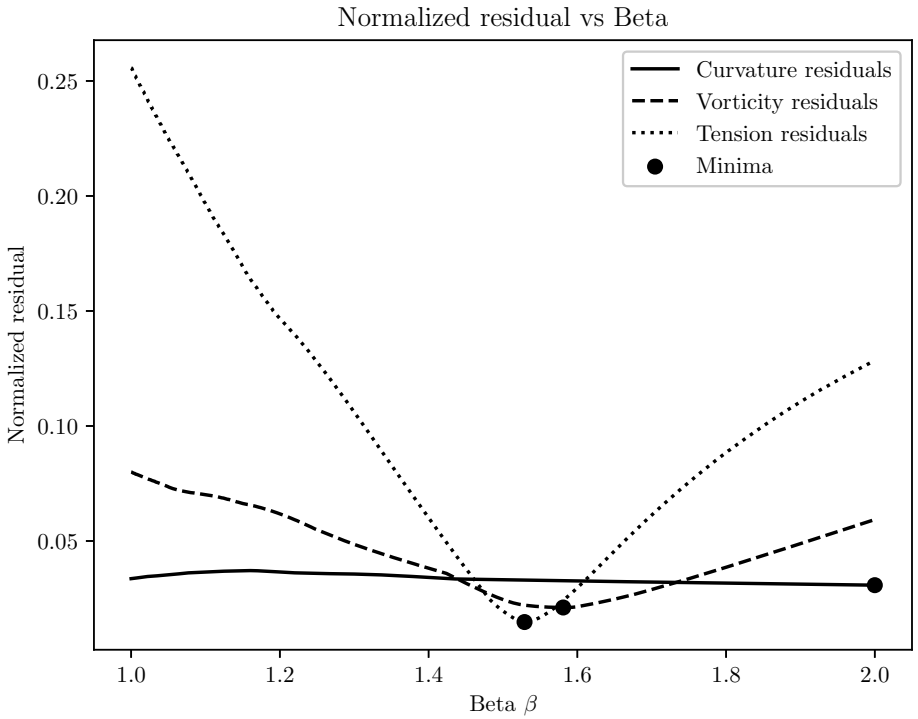

Figure 6: Normalized residuals of curvature, vorticity, and tension from the line of fit on the self-similar region ($\xi \in [3 \cdot 10^{-1}, 4 \cdot 10^4]$) in a scan through β's spaced 0.001 apart. The dots indicate the minimum values for quantities. The minima are 2.000 (curvature), 1.581 (vorticity), and 1.529 (tension).

Despite the curvature not minimizing on the interior of this region of β's, the range of the curvature residuals is 0.0063, when their mean is an order of magnitude larger at 0.0336 ± 0.0020.

2.3 Fitting the loop

On first glance, the loops presented in Figure 4 appear to have the same uniformly scaled profile over time. Consequently, we introduce the profile (X, Y) rescaled by some function $S(\tau)$.

$$(X, Y) = S(\tau)(x, y) \qquad \tau = T - t \tag{25}$$

The profile seen in Figure 4 resembles the algebraic curve $X^2 + Y(Y - \mu)^2 = 0$, which can be parametrized as

$$(X(\xi), Y(\xi)) = (\xi^3 + \mu\xi, -\xi^2) \tag{26}$$

for some $\mu < 0$.

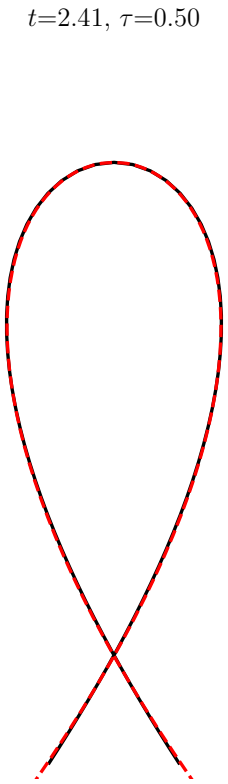

Figure 7: Fitted curve (red, dashed) of (26) plotted against the unit length chain (black, solid) at $t = 2.41$ or $\tau = 0.50$.

With the profile alone, we could study the tangential angle ϕ and curvature k. However with the numerical evidence for the self-similar variable $\xi = s\tau^{-\beta}$, we can also study the vorticity ω.

$$\phi = \arctan\left(\frac{y'}{x'}\right) = \arctan\left(\frac{-2\xi}{3\xi^2+\mu}\right) \tag{27}$$

$$k = \frac{x'y'' - y'x''}{((x')^2 + (y')^2)^{3/2}} = \frac{2}{S(\tau)} \frac{-3\xi^2+\mu}{(9\xi^4 + (6\mu+4)\xi^2 + \mu^2)^{3/2}} \tag{28}$$

$$\omega = \beta S(\tau)\tau^{-1}\xi k = \frac{2\beta}{\tau} \frac{-3\xi^3+\mu\xi}{(9\xi^4 + (6\mu+4)\xi^2 + \mu^2)^{3/2}} \tag{29}$$

The maximum curvature occurs at $\xi = 0$.

$$k_{\max} = \frac{2}{S(\tau)\mu^2} \, . \tag{30}$$

Comparing the curvature scaling expected from equation (22) and above, we conclude that $S(\tau) = C\tau^{\beta}$ for some constant C.

Using the data from the simulation, we fit for C and μ.

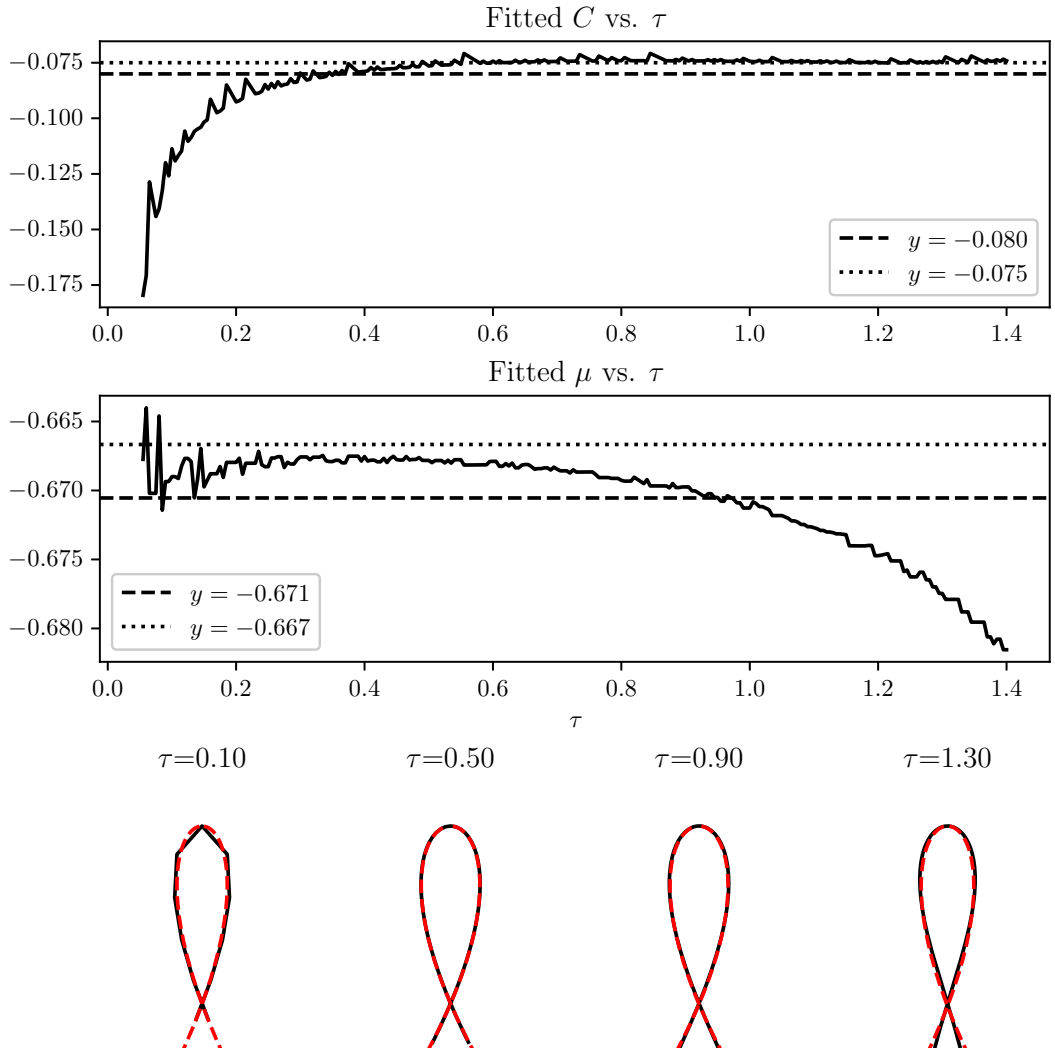

Figure 8: Fits (black, dashed) of C (top) and μ (middle) to a sample over time of the curve where $\beta = 1.5$. To read the C and μ graphs forward in time, read from right to left. Below are the rescaled views of the loop (black, solid) and the fit (red, dashed) at a $\tau = 0.1$, 0.5, 0.9, and 1.3.

From the fits, $C = -0.08 \pm 0.001$ and $\mu = -0.671 \pm 0.0002$. If $\mu \to 0$ as $\tau \to 0$, then that would have indicated a cusp. However $\mu \nrightarrow 0$ still allows for a corner instead.

Using the tension equation (8), one could go further and attempt to solve for the tension, but the differential equation becomes quite hairy.

3 Post-blow up evolution

In the simulation, the blow up does not occur because the chain is a system of ordinary differential equations, and equations (35), (36), and (37) depend on finite differences instead of derivatives.

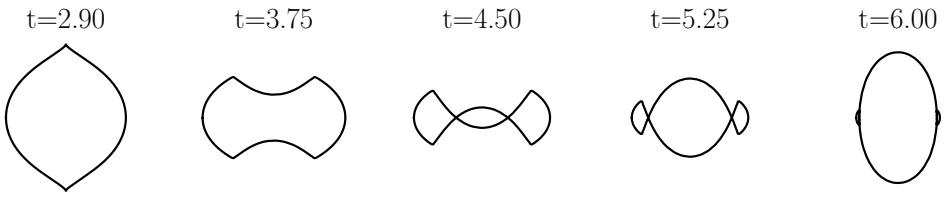

Figure 9: Evolution of the chain after the blow up from the numerical simulation ($M = 1000$ links)

We notice that there appear to be 'shockwaves' that propagate out from the singular points. When comparing the $M = 1000$ link simulation with the $M = 200$ link simulation, the corners become 'sharper,' suggesting that these jump discontinuities in the tangent vector or weak shocks may be singularities in the continuous limit.

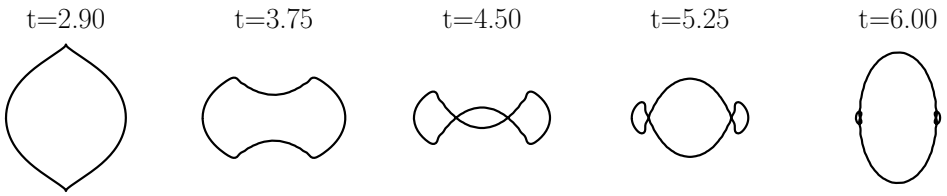

Figure 10: Evolution of the chain after the blow up from the numerical simulation ($M = 200$ links)

The consistency of the numerical method post-blow up suggests that unique continuation after the blow up time is possible and that it may contain propagating singularities. This possibility of dissipative generalized solutions was discussed by Shnirelman in [6].

Conjecture 1. *There exist solutions to the Cauchy problem of equation* (2) *in the weak sense where the constraint* (1) *holds almost everywhere.*

3.1 Curvature behavior

Based on the definition of curvature in Section 1.2, we expect the curvature to stay constant through evolution up to the singular time.

This is similar in spirit to the Whitney-Graustein theorem and the notion of a regular homotopy from differential geometry[1].

Let X be the space of regular curves in $\mathbb{R}^2$. Two regular curves C_0, C_1 are *regularly homotopic* if and only if there exists a continuous map $h : [0, 1) \to X$ such that $h(0) = C_0$, $h(1) = C_1$, and $\forall t \in [0, 1), h(t) \in X$.

The Whitney-Graustein theorem states that two closed, regular curves are regularly homtopic if and only if they have the same rotation index [8], where the rotation index n of a closed regular curve $x \in X$ is defined as

$$2\pi n = \int_0^1 k(s)ds \tag{31}$$

as in [2] on page 38. The result is similar to knowing that the curvature for our periodic string constant. However, our string is allowed to be as irregular as C^2 instead of smooth but is restricted by the dynamics given by (2) instead of just any homotopy with non-vanishing first derivative.

Another differential geometry theorem is Fenchel's theorem which states that a closed regular curve has total absolute curvature greater than or equal to 2π

$$2\pi \leq \int_0^1 |k(s)|\, ds$$

with equality only for convex curves [2]. This means that we expect the curve to have constant total absolute curvature while it is convex, but to have larger total absolute curvature afterwards.

[1] Definitions of differentiable (smooth), regular, closed, and convex plane curves can be found in a standard differential geometry textbook such as do Carmo's book [2] on pages 2, 6, 32, and 39 respectively.

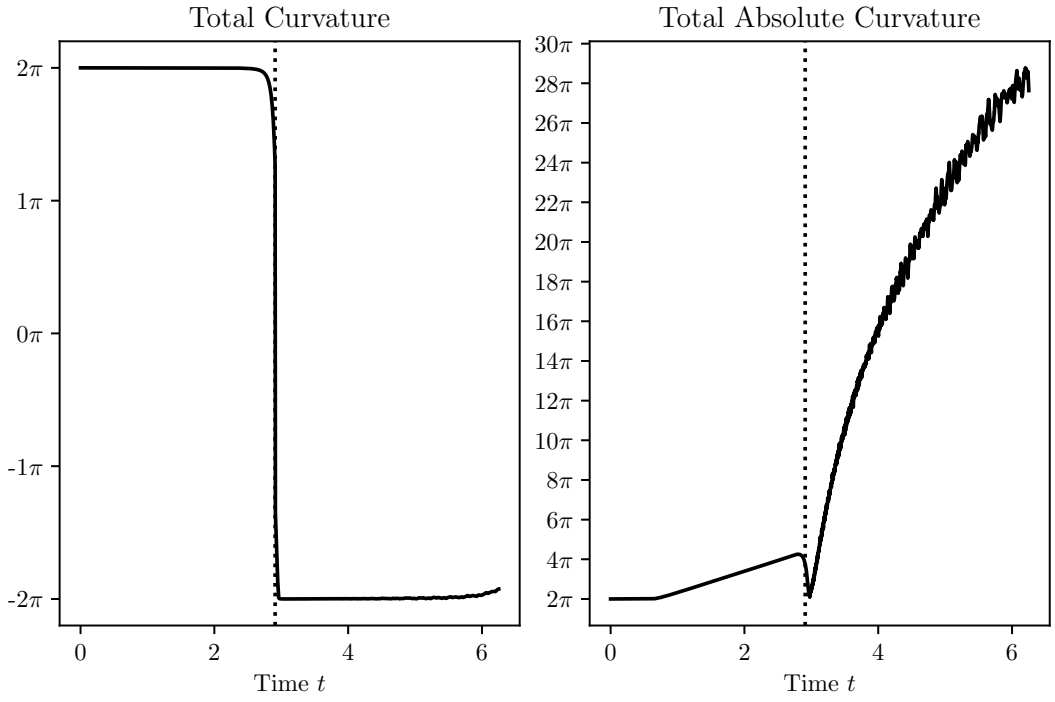

Figure 11: The left plot shows the total absolute curvature against time, and the right plot shows the total curvature against time. The first vertical line on both is when the string stops being convex, and the second vertical line is the blow up time.

In the numerical simulation of the chain, we observe the expected behavior from Fenchel's and the Whitney-Graustein theorems. If the curve after the blow up time was regular, we would expect it to have a rotation index $n = -1$ and have a constant -2π total signed curvature as observed. However, the curve after the blow up is suspected to be some kind of weak solution with a discontinuous first derivative.

3.2 Energy behavior

We are interested in if energy is conserved after the blow up. In Section A.2, we show that energy is conserved for smooth solutions. Checking this numerically, we see that energy conservation holds in the simulation up until the blow up time. For a chain with M links of size Δs, the discrete energy is defined as

$$E(t) = \frac{1}{2} \sum_{i=1}^{M} \Delta s \left\| \partial_t x_{i+1} \right\|^2 \tag{32}$$

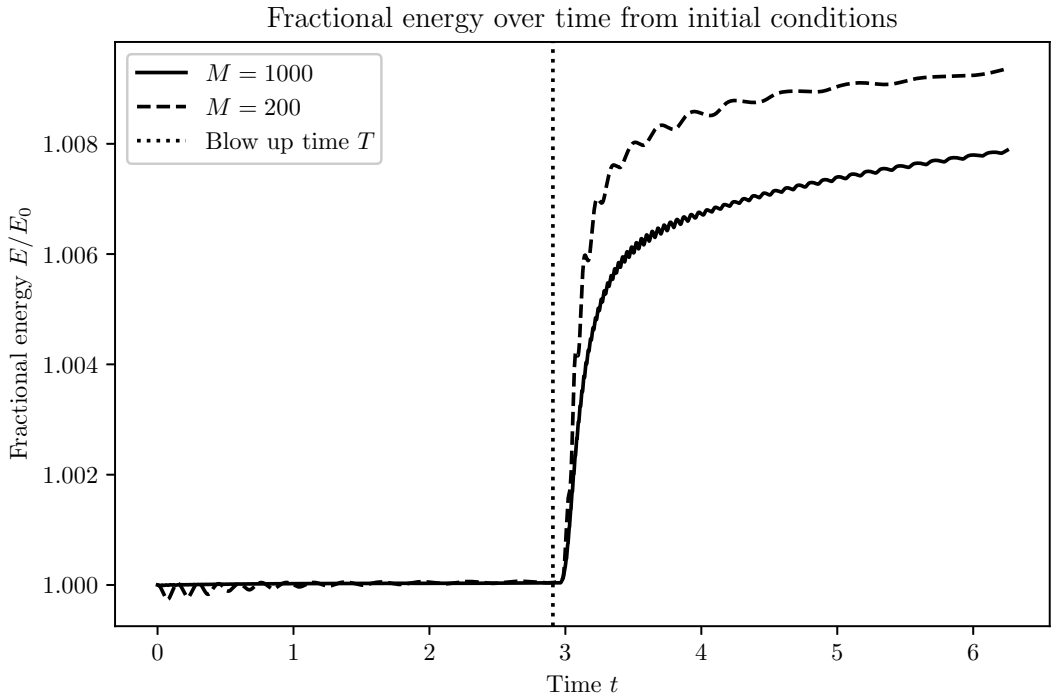

Figure 12: Plot of the energy over time in the numerical simulation for unit length chain with $M = 200$ and $M = 1000$ links.

Some time after the blow up, energy seems to grow This is unphysical. In fact, it has been commented that, under some generalized notion, solutions may be able to lose energy [6]. This means either energy is not conserved after blow up or that the simulation is inaccurate at this point. To get a better idea of either, a proof or counterexample would need to be provided for energy conservation of weak solutions or more simulations with progressively higher resolutions would need to be performed.

4 Discussion

In this write-up, most of the numerical results from Thess et al. about the inextensible periodic string have been reproduced, and we offer a classification of the singularity as a corner.

What remains to be shown is deeper analysis of the tension σ. The motion of inflection points and the self-similar analysis of the profile $X^2 + Y(Y-\mu)^2 = 0$ suggests that the singularity is a corner instead of a cusp.

While we have analyzed inflection points of the curve, we haven't studied zeros of vorticity and the importance of $\partial_s \omega$ at said zeros. We note that in the simualtion, at the singular points $\omega = 0$ and $\partial_s \omega > 0$, while at the 'waist' of the curve $\omega = 0$ as well, but $\partial_s \omega < 0$. The periodicity of ω and conservation of total curvature encapsulates the information that more bending in one spot on the string means bending less somewhere else.

Finally, we note that the energy growth after the blow up is unexpected. Under the analogy that the string is similar to fluids, one may expect to see a decrease in the energy, but instead it increases. Explicit numerical schemes exhibit this instability on time scales too small for the chosen step size, and the chosen Euler method is only first order. Qualitatively, the curvature and vorticity are wildly discontinuous on the curve behind the propagating 'near-'singularities after the blow up. This suggests that the spatial resolution is also too limited. This is the only major inconsistency between the simulation and the theorems proven, and it is rather miraculous in fact that such good consistency between the numerics and analytics is otherwise observed for such low-resolution, low-order numerics. An implicit numerical method may remove this error at the cost of more expensive calculations and inaccurate energy dissipation as opposed to growth.

The periodic boundary condition case for the thin, inextensible string is an exciting problem for future work at the advanced undergraduate/early graduate level. Future work might be to prove local existence for the periodic boundary condition as Preston had done for the two free ends and whip boundary conditions in [4].

Acknowledgements I thank my advisor Professor Theodore Drivas for his ongoing encouragement, support, and insight throughout the project. Additionally, I would like to thank Daniil Glukhovskiy for his help with the velocity constraint, specifically (39) and (41). I would like to thank my friend Leslie Yan for interesting discussions on the physical intuition of the string. I express

my gratitude for the Summer Math Foundation for funding this project.

A Appendix

A.1 Derivation of equation of motion (2)

The equation of motion (2) can be derived using the Lagrangian formalism of mechanics. The constrained Lagrangian density is given below.

$$\mathscr{L} = \frac{1}{2}\rho(s)\left\|\partial_t x(s,t)\right\|^2 \qquad \left\|\partial_s x(s,t)\right\| = 1$$

By the method of Lagrange multipliers, the constrained Lagrangian density can be transformed into an unconstrained Lagrangian density with a Lagrange multiplier $\frac{1}{2}\sigma(s,t)$.

$$\mathscr{L} = \frac{1}{2}\rho(s)\partial_t x(s,t)^2 - \frac{1}{2}\sigma(s,t)(1 - \left\|\partial_s x\right\|^2)$$

Under the principle of least action, we take the variational derivative of the action $S[x(s,t)] = \int_0^1 \int_{t_1}^{t_2} \mathscr{L} dtds$ and set it to 0 to obtain a stationary point.

$$S[x(s,t)] = \int_0^1 \int_{t_1}^{t_2} \left(\frac{1}{2}\rho(s)\left\|\partial_t x(s,t)\right\|^2 - \frac{1}{2}\sigma(s,t)(1 - \left\|\partial_s x(s,t)\right\|^2)\right) dtds$$

$$\delta S[x(s,t)] = 0 = \int_0^1 \int_{t_1}^{t_2} \left(\langle \rho(s)\partial_t x(s,t), \delta\partial_t x(s,t)\rangle - \sigma(s,t)\langle \partial_s x(s,t), \delta\partial_s x(s,t)\rangle\right) dtds$$

Apply integration by parts to shift the derivatives off of $\delta\partial_t x$ and $\delta\partial_s x$.

$$\begin{aligned} 0 = &\int_0^1 \int_{t_1}^{t_2} \langle \rho(s)\partial_{tt} x(s,t) - \partial_s(\sigma(s,t)\partial_s x(s,t)), \delta x(s,t)\rangle dtds \\ &- \int_0^1 \langle \rho(s)\partial_t x(s,t), \delta x(s,t)\rangle|_{t_1}^{t_2}\, ds - \int_{t_1}^{t_2} \langle \partial_s x(s,t), \delta x(s,t)\rangle|_0^L\, dt \\ 0 = &\int_0^1 \int_{t_1}^{t_2} \langle \rho(s)\partial_{tt} x(s,t) - \partial_s(\sigma(s,t)\partial_s x(s,t)), \delta x(s,t)\rangle dtds \end{aligned}$$

By the calculus of variations, the integrand is zero $\forall s \in [0,1)$ and $\forall t$ where $\partial_t x$ exists. From this, the equation of motion is derived.

$$\begin{aligned} 0 &= \rho(s)\partial_{tt} x(s,t) - \partial_s(\sigma(s,t)\partial_s x(s,t)) \\ \boxed{\rho(s)\partial_{tt} x(s,t) &= \partial_s(\sigma(s,t)\partial_s x(s,t))} \end{aligned}$$

In this, we only consider the uniform string, $\rho(s) = 1$.

$$\partial_{tt}x(s,t) = \partial_s(\sigma(s,t)\partial_s x(s,t))$$

A.2 Conserved quantities

Several quantities are conserved for smooth solutions of the non-uniform, thin, inextensible string. These correspond to continuous symmetries in the string. The mass density is $\rho(s) > 0$. The equation of motion reduces to (2) when the linear mass density is uniform $\rho(s) = 1$.

$$\rho(s)\partial_{tt}x(s,t) = \partial_s(\sigma(s,t)\partial_s x(s,t)) \tag{33}$$

The conserved quantities for smooth solutions are

$$\begin{aligned}
\partial_t \int_0^1 \frac{1}{2}\rho(s)[\partial_t x(s,t)]^2 ds = 0 && \text{(Energy)} \\
\partial_t \int_0^1 \rho(s)\partial_t x(s,t) ds = 0 && \text{(Linear momentum)} \\
\partial_t \int_0^1 \rho(s)\partial_t x(s,t) \cdot x^{\perp}(s,t) ds = 0 && \text{(Angular momentum)}
\end{aligned} \tag{34}$$

Additionally, in the uniform string $\rho(s) = 1$, circulation is also conserved.

$$\partial_t \int_0^1 \partial_t x(s,t) \cdot \partial_s x(s,t) ds = 0 \qquad \text{(Circulation)}$$

The circulation is only conserved for the uniform string because the continuous symmetry in s is broken if the string is not uniform $\rho(s) = 1$ i.e. an impulse on a heavier part of a string has a different effect than an impulse on a lighter section.

Proof. Functional dependencies are removed for clarity. ρ is not time-dependent. For energy,

$$\begin{aligned}
\partial_t \int_0^1 \frac{1}{2}\rho[\partial_t x]^2 ds &= \int_0^1 \rho\partial_{tt}x \cdot \partial_t x ds \\
\int_0^1 \partial_t x \cdot \partial_s(\sigma\partial_s x) ds &= -\int_0^1 \partial_{st}x \cdot \sigma\partial_s x ds = 0
\end{aligned}$$

For linear momentum,

$$\partial_t \int_0^1 \rho \partial_t x ds = \int_0^1 \partial_s(\sigma \partial_s x) ds = 0$$

For angular momentum,

$$\partial_t \int_0^1 \rho(\partial_t x \cdot x^\perp) ds = \int_0^1 \partial_s(\sigma \partial_s x) \cdot x^\perp ds = \int_0^1 \partial_s(\sigma \partial_s x \cdot x^\perp) ds = 0$$

For circulation in the uniform case,

$$\begin{aligned} \partial_t \int_0^1 \partial_t x \cdot \partial_s x ds &= \int_0^1 \partial_{tt} x \cdot \partial_s x + \partial_t x \cdot \partial_{st} x ds \\ &= \int_0^1 \partial_s \sigma ds + \int_0^1 \frac{1}{2} \partial_s \left\| \partial_t x \right\|^2 ds = 0 \end{aligned}$$

□

Note that this does not say anything about conservation with shocks like those seen in Section 3 or through the singularity in the last panel of Figure 1.

A.3 Finite approximation and simulation

The numerical simulation is based off the finite approximation of the string by a discrete chain. In Preston's paper [4], he proves that the motion of the chain approaches the string in the discrete to continuous limit in order to prove uniqueness and existence for solutions for the string in short times.

Here, we use the chain equations for simulation as, Preston did in [1]. This turns the tension equation into a matrix equation (37).

For the rest of the simulation details, time-evolution is discretized by a simple Euler method, and the choice of initial conditions is similar to those in Thess et al. [7]. The difference in initial conditions is discussed in Section A.4. The initial conditions used are from the caption of Figure 1.

$$\begin{aligned} x(s,0) &= \cos(s) e_x + \sin(s) e_y \\ \partial_t x(s,0) &= -2/30 \cos^3(s) e_x + 2/30 \sin^3(s) e_y \end{aligned}$$

The combination of discrete time steps and Preston's chain scheme make it so the blow up time and configuration are effectively "skipped" over. While its accuracy compared to the string is questionable, post-"blow up" evolution is possible resulting in what appear to be shocks.

A.3.1 Derivation of chain equation of motion

Consider a periodic chain of length 1 constructed out of n joints $(x_1, \ldots, x_n)$ connected by uniform, rigid link of length $\Delta s = \frac{1}{n}$. As a periodic chain, the indices are periodic with period n. For clarity let $q = (x_1, \ldots, x_n)$ and $\partial_t q = (\partial_t x_1, \ldots, \partial_t x_n)$ when expressing the degrees of freedom of the system.

The Lagrangian L of the system is a function of the position and velocity.

$$\begin{aligned} L(q, \partial_t q) &= \frac{1}{2} \sum_{i=1}^{n} |\partial_t x_i(t)|^2 \\ \forall i \in \mathbb{Z} \quad & |x_{i+1} - x_i| = \Delta s \\ \forall i \in \mathbb{Z} \quad & x_i(t) = x_{i+n}(t) \end{aligned}$$

We add the discretized non-stretch constraint to form the constrained Lagrangian. Let the $\sigma_i(t)$ be the i-th Lagrange multiplier for the i-th constraint.

$$L(q, \partial_t q) = \sum_{i=1}^{n} \left(\frac{1}{2} |\partial_t x_i(t)|^2 - \frac{1}{2} \sigma_i(t) \left(1 - \left\| \frac{x_{i+1}(t) - x_i(t)}{\Delta s} \right\|^2 \right) \right)$$

This defines the action S between times t_1 and t_2 as

$$S[q] = \int_{t_1}^{t_2} \sum_{i=1}^{n} \left(\frac{1}{2} \|\partial_t x_i(t)\|^2 - \frac{1}{2} \sigma_i(t) \left(1 - \left\| \frac{x_{i+1}(t) - x_i(t)}{\Delta s} \right\|^2 \right) \right) dt$$

To find a stationary point of the action, take the variational derivative and set it equal to 0.

$$\delta S[q] = 0 = \int_{t_1}^{t_2} \sum_{i=1}^{n} \left(\partial_t x_i(t) \cdot \delta \partial_t x_i(t) + \sigma_i(t) \left(\frac{x_{i+1}(t) - x_i(t)}{(\Delta s)^2} \cdot \delta (x_{i+1}(t) - x_i(t)) \right) \right) dt$$

Apply integration by parts to shift the derivative off of $\delta \partial_t x$ and expand dot

products into separate sums.

$$
\begin{aligned}
0 = \int_{t_1}^{t_2} \Bigg(& \sum_{i=1}^{n} \left(\partial_{tt} x_i(t) - \frac{\sigma_i(t)}{(\Delta s)^2} (x_{i+1}(t) - x_i(t)) \cdot \delta x_i(t) \right) \\
& + \sum_{i=1}^{n} \left(\frac{\sigma_i(t)}{(\Delta s)^2} (x_{i+1}(t) - x_i(t)) \cdot \delta x_{i+1}(t) \right) \Bigg) dt \\
& - \sum_{i=1}^{n} (\partial_t x_i(t) \cdot \delta x_i(t))|_{t_1}^{t_2} \\
= \int_{t_1}^{t_2} \Bigg(& \sum_{i=1}^{n} \left(\partial_{tt} x_i(t) - \frac{\sigma_i(t)}{(\Delta s)^2} (x_{i+1}(t) - x_i(t)) \cdot \delta x_i(t) \right) \\
& + \sum_{i=1}^{n} \left(\frac{\sigma_i(t)}{(\Delta s)^2} (x_{i+1}(t) - x_i(t)) \cdot \delta x_{i+1}(t) \right) \Bigg) dt
\end{aligned}
$$

Shift the indices of the second summation and combine the two summations.

$$
\begin{aligned}
0 = \int_{t_1}^{t_2} \Bigg(& \sum_{i=1}^{n} \left(\partial_{tt} x_i(t) - \frac{\sigma_i(t)}{(\Delta s)^2} (x_{i+1}(t) - x_i(t)) \right) \cdot \delta x_i(t) \\
& + \sum_{i=1}^{n} \left(\frac{\sigma_{i-1}(t)}{(\Delta s)^2} (x_i(t) - x_{i-1}(t)) \right) \cdot \delta x_i(t) \Bigg) dt \\
= \int_{t_1}^{t_2} & \sum_{i=1}^{n} \left(\partial_{tt} x_i(t) - \left(\frac{\sigma_i(t)}{(\Delta s)^2} (x_{i+1}(t) - x_i(t)) - \frac{\sigma_{i-1}(t)}{(\Delta s)^2} (x_i(t) - x_{i-1}(t)) \right) \right) \cdot \delta x_i(t) dt \\
= \sum_{i=1}^{n} \int_{t_1}^{t_2} & \left(\partial_{tt} x_i(t) - \left(\frac{\sigma_i(t)}{(\Delta s)^2} (x_{i+1}(t) - x_i(t)) - \frac{\sigma_{i-1}(t)}{(\Delta s)^2} (x_i(t) - x_{i-1}(t)) \right) \right) \cdot \delta x_i(t) dt
\end{aligned}
$$

By expanding the inner product and applying the fundamental lemma of the calculus of variations term-wise, the summation in the integrand of each term is 0. This immediately yields the desired equation of motion for each link.

$$
\begin{aligned}
0 &= \partial_{tt} x_i(t) - \left(\frac{\sigma_i(t)}{(\Delta s)^2} (x_{i+1}(t) - x_i(t)) - \frac{\sigma_{i-1}(t)}{(\Delta s)^2} (x_i(t) - x_{i-1}(t)) \right) \\
\boxed{\partial_{tt} x_i(t) &= \frac{\sigma_i(t)}{\Delta s} \left(\frac{x_{i+1}(t) - x_i(t)}{\Delta s} \right) - \frac{\sigma_{i-1}(t)}{\Delta s} \left(\frac{x_i(t) - x_{i-1}(t)}{\Delta s} \right)} \qquad (35)
\end{aligned}
$$

In this suggestive form, it becomes clear that as the spacing of the joints $\Delta s \to 0$ (equivalently number of joints $n \to \infty$) that the discrete system of the chain approaches that of the string if $x_i(t) \to x(s,t)$ and $\sigma_i(t) \to \sigma(s,t)$. However, this does not prove convergence of the motion, which is done in [4].

A.3.2 Chain tension equation derivation

The tension equation for the chain is also derived in a similar procedure as the tension equation of the string. Due to the lengthy nature of these expressions, the time-dependence of the tension σ_i, position x_i, and velocities $\partial_t x_i$ are suppressed.

Subtract the equations of motion between the $(i+1)$-st and the i-th equations of motion.

$$\begin{aligned}
\partial_{tt}x_{i+1} - \partial_{tt}x_i =& \frac{\sigma_{i+1}}{\Delta s}\left(\frac{x_{i+2}-x_{i+1}}{\Delta s}\right) - \frac{\sigma_i}{\Delta s}\left(\frac{x_{i+1}-x_i}{\Delta s}\right) \\
&- \frac{\sigma_i}{\Delta s}\left(\frac{x_{i+1}-x_i}{\Delta s}\right) + \frac{\sigma_{i-1}}{\Delta s}\left(\frac{x_i-x_{i-1}}{\Delta s}\right) \\
=& \frac{\sigma_{i+1}}{\Delta s}\left(\frac{x_{i+2}-x_{i+1}}{\Delta s}\right) - 2\frac{\sigma_i}{\Delta s}\left(\frac{x_{i+1}-x_i}{\Delta s}\right) \\
&+ \frac{\sigma_{i-1}}{\Delta s}\left(\frac{x_i-x_{i-1}}{\Delta s}\right)
\end{aligned}$$

Take the dot product against the difference between the position of $(i+1)$-st and i-th joint.

$$\begin{aligned}
(\partial_{tt}x_{i+1} - \partial_{tt}x_i)\cdot(x_{i+1}-x_i) =& \sigma_{i+1}\left(\frac{x_{i+2}-x_{i+1}}{\Delta s}\right)\cdot\left(\frac{x_{i+1}-x_i}{\Delta s}\right) \\
&- 2\sigma_i \\
&+ \sigma_{i-1}\left(\frac{x_i-x_{i-1}}{\Delta s}\right)\cdot\left(\frac{x_{i+1}-x_i}{\Delta s}\right)
\end{aligned}$$

Analogously to the continuous string, it can be shown through the product rule that

$$(\partial_{tt}x_{i+1} - \partial_{tt}x_i)\cdot(x_{i+1}-x_i) = -|\partial_t x_{i+1} - \partial_t x_i|^2 \tag{36}$$

Substituting in this relation (36) yields the final form of the chain tension

equation.

$$\boxed{\begin{aligned} -|\partial_t x_{i+1} - \partial_t x_i|^2 = \sigma_{i+1}\left(\frac{x_{i+2}-x_{i+1}}{\Delta s}\right)\cdot\left(\frac{x_{i+1}-x_i}{\Delta s}\right) - 2\sigma_i \\ +\sigma_{i-1}\left(\frac{x_i - x_{i-1}}{\Delta s}\right)\cdot\left(\frac{x_{i+1}-x_i}{\Delta s}\right) \end{aligned}} \tag{37}$$

Notice that the right side is a linear combination of σ_i's. This equation is easily rewritten as a real matrix equation of the form $A\sigma = b$. Here, where A is a diagonally-dominant tri-diagonal coefficient matrix with two additional terms in the upper right and bottom left corners. σ here is a column vector containing the σ_i's. b is a vector containing the LHS of the boxed final form of the chain tension equation.

A.4 The velocity constraint

In the chain simulation, the initial conditions must meet the chain equivalent of the velocity constraint.

$$\partial_s x \cdot \partial_{st} x = 0 \qquad (x_{i+1} - x_i) \cdot (\partial_t x_{i+1} - \partial_t x_i) = 0 \tag{38}$$

or else the chain will stretch over time. I suspect that this has to do with its inclusion in the tension equation (8) (or (37)) derivation, but nonetheless, we are limited to simulating systems with compatible initial velocities. This seems to not be a limitation for Thess et al. [7] or Preston [1] who used the following initial conditions

$$x(s,0) = (\cos(s), \sin(s)) \qquad \partial_t x(s,0) = (-c\cos(s), c\sin(s)) \tag{39}$$

up to a constant c scaling the initial velocities.

$$\partial_s x \cdot \partial_{st} x = (\cos(s), \sin(s)) \cdot (-c\cos(s), c\sin(s)) \tag{40}$$
$$= c(\sin^2(s) - \cos^2(s)) \tag{41}$$

One can see above that the velocity constraint is not met.

If we assume that the initial conditions are smooth, then we can write them as a Fourier series

$$x(s,0) = \sum_{n\in\mathbb{Z}} x_n e^{i2\pi ns} \qquad \partial_t x(s,0) = \sum_n \dot{x}_n e^{i2\pi ns}$$

enforced to be real-valued

$$\forall n \in \mathbb{Z},\ x_n = \overline{x_{-n}},\ \dot{x}_n = \overline{\dot{x}_{-n}}$$

and take their dot product.

By doing this, multiplying both sides by $e^{-i2\pi k}$, and integrating, we find

$$0 = \partial_s x \cdot \partial_{st} x = \sum_{n,m\in\mathbb{Z}} nm(x_n \cdot \dot{x}_m) e^{i2\pi(n+m)s}$$

$$\Rightarrow \boxed{\forall k \in \mathbb{Z},\ 0 = \sum_{n\in Z} n(k-n)(x_n \cdot \dot{x}_{k-n})}$$

References

[1] Stephen C. Preston and Ralph Saxton. An H^1 model for inextensible strings. *Discrete & Continuous Dynamical Systems - A*, 33(5):2065–2083, 2013.

[2] Manfredo Perdigão do Carmo. *Differential geometry of curves and surfaces*. Mathematics. Dover Publications, Inc, Mineola, New York, revised & updated second edition edition, 2016.

[3] James Raymond Munkres. *Analysis on manifolds*. Addison-Wesley, Reading, Mass., 5. print edition, 1994.

[4] Stephen C. Preston. The motion of whips and chains. *Journal of Differential Equations*, 251(3):504–550, August 2011.

[5] Stephen C. Preston. The geometry of whips. *Annals of Global Analysis and Geometry*, 41(3):281–305, March 2012.

[6] Alexander Shnirelman. The motion of an inextensible thread and incompressible fluid and foundations of mechanics. International Conference "Mathematical Hydrodynamics" Abstracts, pages 72–74, Moscow, Russia, June 12-17 2006.

[7] A. Thess, O. Zikanov, and A. Nepomnyashchy. Finite-time singularity in the vortex dynamics of a string. *Physical Review E*, 59(3):3637–3640, March 1999.

[8] Hassler Whitney. On regular closed curves in the plane. *Compositio Mathematica*, 4:276–284, 1937. Series Title: Contemporary Mathematicians.